

Kewu Huang, Wayne Mitzner, Richard Rabold, Brian Schofield, Hannah Lee, Shyam Biswal and Clarke G. Tankersley

J Appl Physiol 102:1632-1639, 2007. First published Jan 11, 2007; doi:10.1152/jappphysiol.00833.2006

You might find this additional information useful...

This article cites 43 articles, 24 of which you can access free at:

<http://jap.physiology.org/cgi/content/full/102/4/1632#BIBL>

This article has been cited by 2 other HighWire hosted articles:

Apoetm1Unc mice have impaired alveologenesis, low lung function, and rapid loss of lung function

D. Massaro and G. D. Massaro

Am J Physiol Lung Cell Mol Physiol, May 1, 2008; 294 (5): L991-L997.

[\[Abstract\]](#) [\[Full Text\]](#) [\[PDF\]](#)

Global expression profiles from C57BL/6J and DBA/2J mouse lungs to determine aging-related genes

V. Misra, H. Lee, A. Singh, K. Huang, R. K. Thimmulappa, W. Mitzner, S. Biswal and C. G. Tankersley

Physiol Genomics, November 14, 2007; 31 (3): 429-440.

[\[Abstract\]](#) [\[Full Text\]](#) [\[PDF\]](#)

Updated information and services including high-resolution figures, can be found at:

<http://jap.physiology.org/cgi/content/full/102/4/1632>

Additional material and information about *Journal of Applied Physiology* can be found at:

<http://www.the-aps.org/publications/jappl>

This information is current as of August 11, 2008 .

Variation in senescent-dependent lung changes in inbred mouse strains

Kewu Huang, Wayne Mitzner, Richard Rabold, Brian Schofield, Hannah Lee, Shyam Biswal, and Clarke G. Tankersley

Johns Hopkins Bloomberg School of Public Health, Department of Environmental Health Sciences, Baltimore, Maryland

Submitted 28 July 2006; accepted in final form 10 January 2007

Huang K, Mitzner W, Rabold R, Schofield B, Lee H, Biswal S, Tankersley CG. Variation in senescent-dependent lung changes in inbred mouse strains. *J Appl Physiol* 102: 1632–1639, 2007. First published January 11, 2007; doi:10.1152/jappphysiol.00833.2006.— Previous studies from our laboratories showed lung development differences between inbred strains of mice. In the present study, the C57BL/6J (B6) and DBA/2J (D2) strains were examined for senescent-dependent differences with respect to the lung structure and function. Specifically, we hypothesize that senescent changes in lung vary between strains due to identifiable gene expression differences. Quasi-static pressure-volume curves and respiratory impedance measurements were performed on 2- and 20-mo-old B6 and D2 mice. Lung volume at 30 cmH₂O (V_{30}) pressure was significantly ($P < 0.01$) increased with age in both strains, but the increase was proportionally greater in D2 (68%) than in B6 (40%) mice. In addition, decreased elastic recoil pressure at 50% of V_{30} and a reduction in airway resistance as a function of positive end-expiratory pressure were observed in 20-mo-old D2 mice but not in B6 mice. Morphometric analysis of lung parenchyma showed significant decreases in elastic fiber content with age in both strains, but the collagen content was significantly ($P < 0.01$) increased with age in D2 but not B6 mice at 20 mo. Furthermore, using quantitative RT-PCR methods, gene expression differences between strains suggested that D2 mice significantly ($P < 0.05$) downregulated the expressions of elastin (*Eln*) and procollagen I, III, and VI (*Col1a1*, *Col3a1*, and *Col6a3*) in lung tissue at 20 mo of age. These age-dependent changes were accompanied by an increased gene expression in matrix metalloproteinase 9 (*Mmp9*) in D2 and an increase in tissue inhibitor of matrix metalloproteinase (*Timp1* and *Timp4*) in B6 mice. In conclusion, the results from the present study demonstrate that lung mechanics of both strains show significant age-dependent changes. However, changes in D2 mice are accelerated relative to B6 mice. Moreover, gene expression differences appear to be involved in the strain-specific changes of lung mechanic properties.

C57BL/6J; DBA/2J; aging; lung mechanics; extracellular matrix

AGING EFFECTS on lung structure and mechanics in humans have been investigated and reviewed in several previous reports (6, 27, 40). In general, senescent-dependent changes in lung mechanics are summarized by a reduction in lung elastic recoil and an increase in residual volume in the absence of a change in total lung capacity (TLC) (6). Other studies have demonstrated that progressive decline in lung function with age is variable among individuals, implying that there are genetic determinants involved in the senescent process (5, 34). However, in humans it is difficult to address the interaction between genetic determinants and aging per se since recruiting senescent volunteers without significant exposure to smoking or air pollution is unfeasible. Alternatively, senescent-dependent changes in lung structure and mechanics have been investi-

gated in rodent models. In Sprague-Dawley rats, for example, a leftward shift in the pressure-volume (P-V) curve was observed, and lung elastance was reduced at high lung volume in the aged group (23). Hirai and colleagues (13) showed senescent-dependent increases in static compliance, dynamic compliance, and TLC in a model of accelerated aging. In short, little is known about the effects of aging per se on alveolar architectural structure, the maintenance of extracellular matrix (ECM), and the consequences of senescence on lung mechanics in humans or in animal models. In particular, the interactive effects between genetic predisposition and aging on lung structure have not been studied.

Numerous studies have shown substantial variation in lung structure and mechanics among inbred mouse strains (16, 30, 38). A comparison of lung structure in male C57BL/6J (B6) and DBA/2J (D2) mice, for example, showed that D2 mice had a larger alveolar air proportion, smaller mean chord length (MCL) of ducts, and smaller fixed lung volume per fresh lung weight (16). These observations lead to a difference in the recoil properties of the lung between the two mouse strains. In addition, B6 and D2 inbred mice have been routinely used to study lung pathophysiological effects of exposure to cigarette smoke (4), bleomycin (7), ozone (32), mycobacterium (2), and allergen (43). These two strains have been shown to be widely different in their genetic characteristics. However, little information is available on the effects of aging per se in altering lung structure and mechanics in these two strains. Therefore, the purpose of this study is to investigate the interactive effects of aging and genetic predisposition, which may lead to individual variation in onset and severity of senescent changes in lung mechanics. We hypothesize that the genetic determinants, which regulate strain differences in lung structure and mechanics in younger B6 and D2 mice, are exacerbated with senescence. Furthermore, the interaction between genetic variability and the aging process might accelerate adverse changes in lung structure and mechanics. To address this question, quasi-static P-V curves, positive end-expiratory pressure (PEEP)-dependence of airway and tissue impedance, elastic fiber and collagen content in lung tissue, and gene expression levels related to lung ECM were studied in adult (2 mo) and aged (20 mo) B6 and D2 mice.

METHODS

Animals. Male B6 and D2 strains of mice were purchased from Jackson Laboratories and the aged mouse colonies at the National Institute on Aging. The two strains of mice were studied at 2 and 20 mo of age. The animals were housed in a facility at the Johns Hopkins University School of Public Health. The temperature was maintained

Address for reprint requests and other correspondence: C. G. Tankersley, Div. of Physiology, Bloomberg School of Public Health, The Johns Hopkins Univ., 615 N. Wolfe St., Baltimore, MD 21205 (e-mail: ctankers@jhsph.edu).

The costs of publication of this article were defrayed in part by the payment of page charges. The article must therefore be hereby marked “advertisement” in accordance with 18 U.S.C. Section 1734 solely to indicate this fact.

at $\sim 21.5^{\circ}\text{C}$, and the light-dark cycle was 12:12 h, beginning at 0700. The animals were housed in cages and fed ad libitum with a pelleted stock diet. All procedures were approved by the Johns Hopkins University Animal Care and Use Committee and complied with the American Physiological Society Guidelines.

Respiratory impedance measurements. Animals were anesthetized with intraperitoneal injections of pentobarbital sodium at a dose of 80 mg/kg body wt. After the trachea was cannulated, the mouse was connected via the tracheal cannula to a computer-controlled small animal ventilator (FlexiVent, Montreal, Canada) while in a supine position. All mice were mechanically ventilated with 100% O_2 at 150 breaths/min and a tidal volume of 10 ml/kg, and each animal was paralyzed with an intraperitoneal injection of 0.05 ml succinylcholine (9 mg/ml). Stable breathing in each animal was attained after 3 min, at which time a deep inspiration was applied at an airway pressure of 30 cmH_2O . The impedance of the respiratory system was measured 2 min after the deep inspiration and then fitted by Flexivent software to a constant-phase model (11, 12) to provide measures of airways resistance (R), tissue damping (G), tissue elastance (H), and tissue hysteresivity (η). For the measurement of impedance, a computer-generated volume signal composed of 19 mutually primed sinusoids ranging from 0.25 to 19.625 Hz was applied to the airway opening. Measurements were made at four different PEEP levels of 2, 5, 10, and 15 cmH_2O with 1-min intervals between each PEEP level.

P-V curve. After the impedance measurements, mice were mechanically ventilated with 100% O_2 at a PEEP of 2 cmH_2O for 1 min, and the cannula was sealed with a stopcock for 3 min to degas the lung. Quasi-static P-V curves were then performed ex vivo with the respiratory system intact. The rate of inflation and deflation was standardized by a dual-infusion withdraw pump (model 900-610, Harvard Apparatus, Dover, MA), and the airway pressure was measured by using a differential pressure transducer (model 8510B-2, Endevco). The initial inflation rate was controlled at ~ 0.75 ml/min to ensure that all lung regions opened before being switched to a rate of 2 ml/min for the remaining inflation-deflation maneuvers. The pressure limits of the inflation and deflation airway pressures were 30 and -10 cmH_2O , respectively. The volumes on deflation at 0 cmH_2O (V_0) and 30 cmH_2O (V_{30}) were considered to represent functional residual capacity (FRC) and TLC, respectively. Compliance of the intact respiratory system was computed from the slopes of the P-V relationships between 5 and 0 cmH_2O (Cr_{5-0}) and between 15 and 10 cmH_2O (Cr_{15-10}) on deflation.

MCL of alveoli and lung tissue density. After the P-V curve was completed, the cannulated trachea was connected to a 10- cmH_2O column of Zenker's fixative (mercuric chloride/acetic acid fixative, EM Science, Gibbstown, NJ) for 4 h. To more consistently control the selection of sample sections, only the left lungs were processed and analyzed. We selected lung sections by a standardized procedure as described by Soutiere et al. (36). From the left lung, the top 3-mm section was removed and discarded, and then three serial, 2-mm sections were removed and processed for histology. Blocks were washed in 70% alcohol twice followed by 80% alcohol preservation, then embedded in paraffin in methacrylate. For the measurement of MCL, 5- μm -thick sections were cut and stained with 0.05% toluidine blue. From each section, seven nonoverlapping 676 $\mu\text{m} \times 505 \mu\text{m}$ fields were sampled, deliberately avoiding the large airways and blood vessels. Each of these regions was photographed for digital analysis, and conventional morphometric methods were used to determine MCL of alveoli using NIH Image software (version 1.62). For consistency with previous studies (36), chord lengths $< 8 \mu\text{m}$ or $> 250 \mu\text{m}$ were excluded. The lung tissue density (T_D) was computed as the percentage of the total area of the lung tissue divided by the total area of the histological field. Like the MCL measurements, 21 histological samples were obtained from each animal and averaged for a given animal.

Quantification of elastic fiber and collagen content. From these same tissue blocks, additional 5- μm sections were analyzed for elastic

fiber and collagen content in lung parenchymal tissue. Sections were stained with acid orcein alcoholic solution for elastic fiber content, and additional sections were stained with 0.05% fast green FCF and picrosirius red for collagen content. Seven nonoverlapping 676 $\mu\text{m} \times 505 \mu\text{m}$ fields were sampled, deliberately avoiding the large airways and blood vessels. To quantify elastic fiber and collagen content in the lung parenchyma, color thresholding was performed using Image-pro plus 5.1 software as described elsewhere (10, 26, 31). In the present study, color thresholding was used to separate the histological samples into pixels associated with different tissue staining procedures. Each image, stained for either elastic fibers or collagen, was composed of contrasting pixels representing the color of interest (i.e., elastic fibers or collagen) against a background color (i.e., other tissue or air space). The areas of elastic fiber [elastic fiber density relative to lung parenchyma (E_{LP})] and collagen [collagen density relative to lung parenchyma (C_{LP})] in the tissue samples were determined by computing the percentage as normalized to the total area of the tissue (10). Twenty-one histological samples were obtained from each animal ($n = 6$ mice per strain for each age group) and averaged for a given animal.

Quantitative RT-PCR. Total RNA isolation was prepared from the lungs of 2- and 20-mo-old B6 and D2 male mice ($n = 3$ per strain per age group) using the TRIzol reagent (Invitrogen, Carlsbad, CA) following the manufacturer's instructions. Total RNA was isolated using the RNeasy Mini Kit (Qiagen, Valencia, CA), and 3 μg of total RNA was reverse transcribed to complementary DNA (cDNA) using random primers and MultiScribe reverse transcriptase (Applied Biosystems, Foster City, CA). Using 100 ng of cDNA as a template, quantification was performed by an ABI Prism 7000 Sequence Detector (Applied Biosystems) using the TaqMan 5' nuclease activity from the TaqMan Universal PCR Master Mix, fluorogenic probes (Applied Biosystems) and oligonucleotide primers (Invitrogen). TaqMan assays were repeated twice for each of 10 selected genes related to lung ECM in each lung sample. These genes were as follows: elastin (*Eln*); procollagen I (*Col1a1*), III (*Col3a1*), and VI (*Col6a3*); matrix metalloproteinase 9 (*Mmp9*) and 12 (*Mmp12*); and tissue inhibitor of metalloproteinase 1 (*Timp1*), 2 (*Timp2*), 3 (*Timp3*), and 4 (*Timp4*). The mRNA expression levels of all samples were normalized to the levels for the housekeeping glyceraldehyde-3-phosphate dehydrogenase (GAPDH) from the same sample, and relative fold changes were calculated using the $2^{-\Delta\Delta C_t}$ method, where C_t is cycle threshold (33).

Statistical analysis. Differences between B6 and D2 mice were analyzed by two-way ANOVA (Graphpad Prism, Version 4.03). Mean comparisons between strains and age groups were further tested by a Bonferroni post test. Statistical significance was accepted at P value of 0.05. Results were expressed as means \pm SE.

RESULTS

The body weight and lung volume parameters are shown in Table 1. There were no detectable differences observed between the strains in body weight within each age group. However, body weight increased significantly with age in both strains of mice ($P < 0.01$). Whereas FRC remained unchanged with age in B6 mice, FRC at 20 mo of age in D2 mice was significantly ($P < 0.01$) increased relative to younger mice, and it was also significantly greater compared with 20-mo-old B6 mice (0.58 ± 0.08 vs. 0.35 ± 0.02 ml, $P < 0.05$). Likewise, the V_{30} increased significantly with age in both strains ($P < 0.01$), but the increase was proportionally greater in D2 (68%) than in B6 (40%) mice. Cr_{5-0} was also increased with age in both strains ($P < 0.01$); however, there were no detectable differences ($P > 0.05$) observed between strains within the same age group. The Cr_{15-10} was increased with age in only B6 mice ($P < 0.01$) and was significantly ($P < 0.01$) lower in D2 compared with B6 mice at both 2 and 20 mo of age.

Table 1. Body weight and lung volume parameters of mice

	B6		D2	
	2 mo (<i>n</i> = 8)	20 mo (<i>n</i> = 7)	2 mo (<i>n</i> = 8)	20 mo (<i>n</i> = 6)
Body weight, g	24.5 ± 0.8	30.6 ± 0.6‡	24.4 ± 1.0	28.3 ± 0.5‡
FRC, ml	0.27 ± 0.03	0.35 ± 0.02	0.30 ± 0.06	0.58 ± 0.08*‡
V ₃₀ , ml	0.97 ± 0.08	1.36 ± 0.02‡	0.84 ± 0.09	1.41 ± 0.07‡
Crs ₅₋₀ , ml/cmH ₂ O	0.042 ± 0.004	0.073 ± 0.003‡	0.039 ± 0.003	0.073 ± 0.005‡
Crs ₁₅₋₁₀ , ml/cmH ₂ O	0.023 ± 0.001	0.028 ± 0.001‡	0.014 ± 0.001†	0.017 ± 0.001†

All values are expressed as means ± SE. B6, C57BL/6J strain; D2, DBA/2J strain; FRC, functional residual capacity = lung volume on deflation at 0 cmH₂O (V₀); V₃₀, lung volume on deflation at 30 cmH₂O; Crs₅₋₀, compliance of the respiratory system between 5 and 0 cmH₂O on deflation; Crs₁₅₋₁₀, compliance of the respiratory system between 15 and 10 cmH₂O on deflation. **P* < 0.05, †*P* < 0.01, D2 vs. B6 at same age; ‡*P* < 0.01, 20 mo vs. 2 mo in same strain.

Figure 1, A and B, shows quasi-static P-V curves normalized to V₃₀ in B6 and D2 mice, respectively. Leftward shifts in the deflation limb of the P-V curves were observed from 2 to 20 mo of age in B6 (*F* statistic_{df=1} = 5.0, *P* < 0.05) and D2 (*F* statistic_{df=1} = 13.1, *P* < 0.01) mice. This shift was quantified by measuring the elastic recoil pressures at 50% of V₃₀ (P_{EL}). The P_{EL} was significantly (*P* < 0.05) lower in D2 compared with B6 mice within the same age group; however, a significant (*P* < 0.05) decrease with age was seen only in D2 mice (3.19 ± 0.61 vs. 1.60 ± 0.48 cmH₂O; Fig. 1C).

The respiratory impedance data at a PEEP level of 2 cmH₂O are shown in Table 2. At 2 mo of age, R was significantly (*P* < 0.01) higher in D2 than in B6 mice, but the strain differences were eliminated in 20-mo-old mice due to a significant (*P* < 0.01) age-dependent decrease in D2 mice. Thus there was a significant interactive effect of age on R between the strains (*F* statistic_{df=1} = 32.23, *P* < 0.001). Both G and H were signif-

icantly (*P* < 0.01) diminished with age in both strains. An age-dependent increase in eta was significant (*P* < 0.01) only in D2 mice.

In Fig. 2A, the strain variation in R is shown for different age groups at increasing levels of PEEP. With increasing PEEP, R progressively decreased in each group. In contrast to B6 mice, D2 mice showed a significant age-dependent decrease in R at all PEEP levels. For example, at a PEEP level of 2 cmH₂O, R was significantly (*P* < 0.01) decreased from 2.29 ± 0.19 to 0.84 ± 0.05 cmH₂O·s/ml from 2 to 20 mo of age in D2 mice. However, R was only slightly (*P* > 0.05) decreased from 0.82 ± 0.05 to 0.74 ± 0.06 cmH₂O·s/ml in B6 mice of similar age. Figure 2B shows the pressure sensitivity of R as a function of increasing PEEP levels. In D2 mice, the pressure sensitivity of R (from 2-cmH₂O to 5-cmH₂O PEEP levels) was significantly (*P* < 0.01) decreased at 20 mo age. There was no age-dependent change in pressure sensitivity of R between 2-

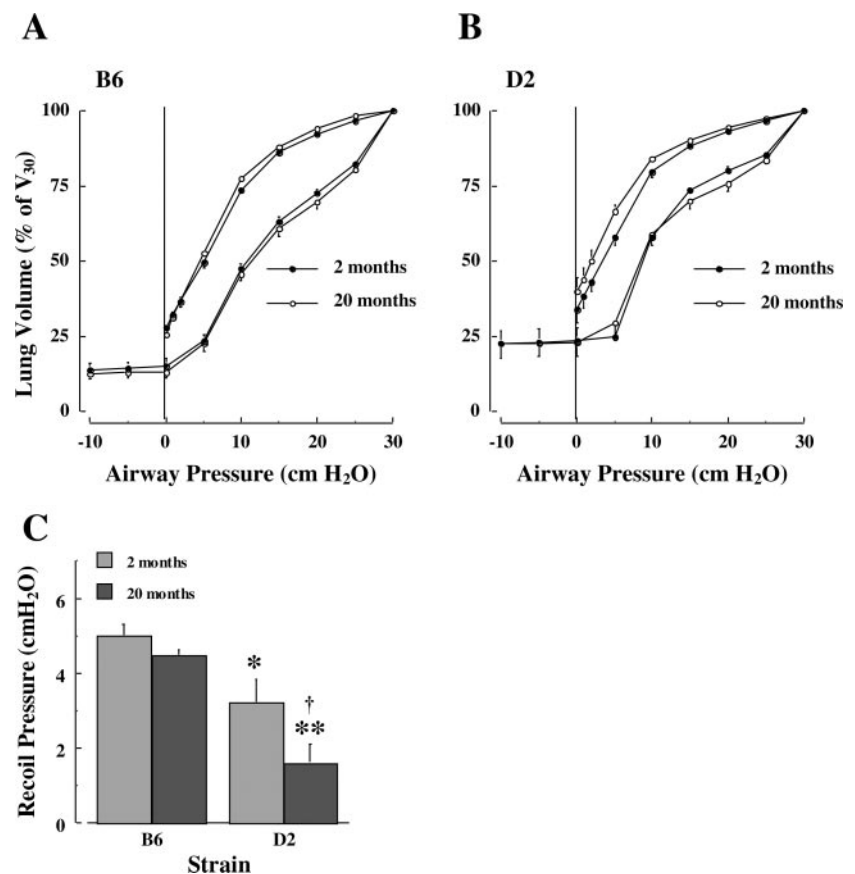


Fig. 1. Static pressure-volume (P-V) curves normalized by the volume achieved at 30 cmH₂O (i.e., percent of V₃₀) in C57BL/6J (B6) (A) and DBA/2J (D2) mouse strains (B). C: changes of elastic recoil pressure at 50% of V₃₀ in both strains of mice. Data are expressed as means ± SE. **P* < 0.05, ***P* < 0.01, D2 vs. B6 at same age; †*P* < 0.05, 20 mo vs. 2 mo in same strain.

Table 2. Respiratory impedance parameters of mice with PEEP of 2 cmH₂O

	B6		D2	
	2 mo (n = 8)	20 mo (n = 6)	2 mo (n = 8)	20 mo (n = 6)
R, cmH ₂ O·s/ml	0.82±0.05	0.74±0.06	2.29±0.19†	0.84±0.05‡
G, cmH ₂ O/ml	6.02±0.29	3.79±0.13‡	5.84±0.33	3.48±0.17‡
H, cmH ₂ O/ml	38.36±1.86	21.08±0.80‡	38.20±2.51	18.06±0.58‡
eta	0.16±0.003	0.18±0.007	0.15±0.008	0.19±0.013‡

All values are expressed as means ± SE. PEEP, positive end-expiratory pressure; R, airways resistance; G, tissue damping; H, tissue elastance; eta, hysteresivity. †*P* < 0.01, D2 vs. B6 at same age; ‡*P* < 0.01, 20 mo vs. 2 mo in same strain.

and 20-mo-old B6 mice (*P* > 0.05). There was also a significant interactive effect of age on the pressure sensitivity of R between the strains (*F* statistic_{df=1} = 20.28, *P* < 0.001). As shown in Fig. 2C, this unique age-dependent change in pressure sensitivity for D2 mice was not exclusively attributable to the elevated R observed in this strain at a younger age.

Figure 3A shows age-dependent changes in alveolar MCL in B6 and D2 mice. The MCL was consistently higher (9–11%) in both strains at 20 mo of age compared with the younger age group (*F* statistic_{df=1} = 5.74, *P* < 0.05). Figure 3B shows the lung T_D in both mouse strains. Although there were no lung T_D differences observed with age in B6 mice, T_D decreased significantly (*P* < 0.05) from 2 mo (33.3 ± 2.1 %) to 20 mo (27.0 ± 1.7 %) of age in D2 mice.

Figure 4 shows age-dependent changes in E_{LP} and C_{LP} for B6 and D2 mice. The E_{LP} decreased significantly (*P* < 0.01) from 2 to 20 mo in both strains (Fig. 4A). However, there were no detectable strain differences observed in E_{LP} within each age group. In Fig. 4B, age-dependent changes in C_{LP} are illustrated. The C_{LP} increased significantly (*P* < 0.01) in D2 mice with age, but the C_{LP} was not significantly (*P* > 0.05) changed with age in B6 mice. In addition, C_{LP} was significantly (*P* < 0.05) higher in D2 mice relative to B6 mice in both age groups.

Table 3 reports age-dependent changes in the gene expression profiles related to lung ECM for B6 and D2 mice. At 20

mo of age, the expression levels of *Colla1*, *Col3a1*, *Col6a3*, and *Eln* genes were significantly (*P* < 0.05) decreased in D2 mice but not in B6 mice. In 2-mo-old mice, the expression level of only the *Colla1*, *Col3a1*, and *Col6a3* genes were significantly (*P* < 0.05) higher in D2 relative to B6 mice. There was also a significant interactive effect of age on the expression levels of the *Col3a1* gene between the strains (*F* statistic_{df=1} = 6.13, *P* < 0.05).

The expression levels of the *Mmp9* gene were modestly increased with age in both strains, but the increase was significantly (*P* < 0.01) greater in 20-mo-old D2 mice. The expression level of the *Timp1* and *Timp4* genes were significantly (*P* < 0.05) increased with age in B6 mice but not in D2 mice. In addition, there were significant interactive effects of age on the expression levels of the *Mmp12* (*F* statistic_{df=1} = 7.56, *P* < 0.05) and *Timp1* (*F* statistic_{df=1} = 14.78, *P* < 0.01) genes between the strains.

DISCUSSION

In the present study, several age-dependent changes occurred in lung mechanics that were common to both B6 and D2 mice, including age-dependent increases in V₃₀ and Crs₅₋₀. In addition, respiratory impedance parameters G and H were also decreased with age in both strains. These common age-dependent changes in both B6 and D2 mice were associated with a decrease in elastin fiber content in the lung parenchyma. On the other hand, there were several notable age-dependent changes unique to the D2 strain. These unique characteristics in D2 mice included decreases in T_D and P_{EL}, which are emphysematous-like changes that are observed with age in humans (41) and other animal models (19). While there were no significant changes in MCL in either strain, the collagen content in D2 mice was significantly elevated at 20 mo of age. These exceptional age-dependent changes in the lungs of D2 mice were accompanied by a substantial reduction in R as a function of PEEP (Fig. 2). Taken together, the results support the hypothesis that D2 mice are characterized by exaggerated age-dependent changes in lung function and structure compared with B6 mice.

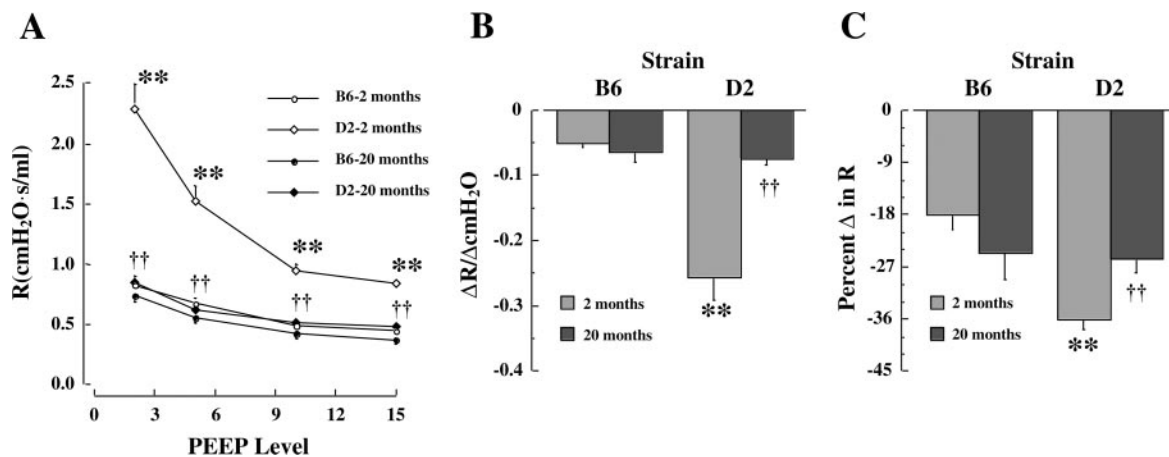


Fig. 2. Airways resistance (R) as a function of increasing levels of positive end-expiratory pressure (PEEP) in B6 and D2 mouse strains. A: airway resistance. B: slope of the relationship between airways resistance as a function of increasing levels of PEEP from 2 to 5 cmH₂O. C: percent change in airways resistance between PEEP levels of 2 cmH₂O and 5 cmH₂O normalized for the resistance at 2 cmH₂O. Data are expressed as means ± SE. ***P* < 0.01 vs. same-age B6 mice. ††*P* < 0.01, 20 mo vs. 2 mo in same strain.

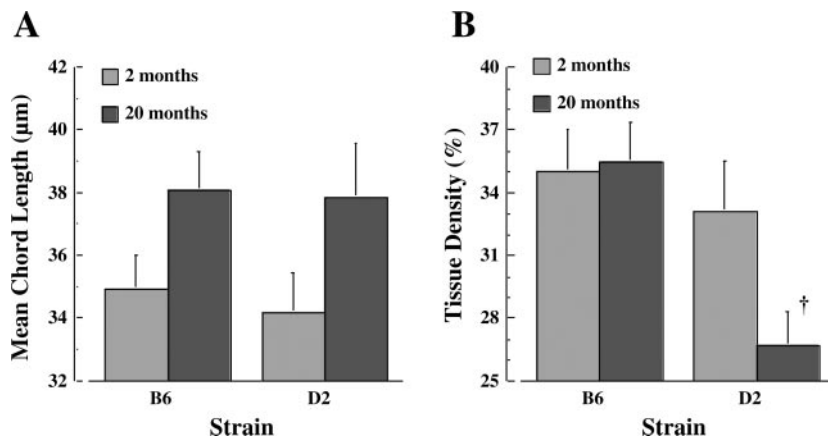


Fig. 3. A: mean chord length (MCL) of alveoli. B: lung parenchymal tissue density (T_D) in B6 and D2 mouse strains. There was consistently higher ($\sim 9\text{--}11\%$) MCL in both strains at 20 mo compared with 2 mo of age (F statistic $_{df=1} = 5.74$, $P < 0.05$). Data are expressed as means \pm SE. † $P < 0.05$, 20 mo vs. 2 mo in same strain.

A similar strain comparison of lung structure was performed in younger male B6 and D2 mice by Kida and coworkers (16). The results observed by these investigators with respect to MCL are relatively similar to those shown in 2-mo-old B6 and D2 from the present study. Our present study quantified many additional structural and mechanical characteristics of the lung between B6 and D2. The most notable strain difference was the measurement of R at relatively low levels of PEEP (Fig. 2). There was a threefold greater R in D2 mice compared to B6 mice. A survey of the literature indicates a broad range of baseline resistances among a variety of inbred strains from 0.3 $\text{cmH}_2\text{O}\cdot\text{s}/\text{ml}$ (1) to 1.5 $\text{cmH}_2\text{O}\cdot\text{s}/\text{ml}$ (35). The variability in baseline R among different studies may be attributable to strain variation or methodological differences, such as variable anesthetic effects and the use of paralyzing agents. The present study also shows that the PEEP dependence of R in 2-mo-old D2 mice was substantially greater than B6 mice. These results indicate that there are robust genetic determinants that regulate the strain variation in R between B6 and D2 mice. Whereas others (18) have shown that the D2 strain is more hyperresponsive to bronchoprovocative agents compared with the B6 mice, these investigators did not measure baseline resistance. In fact, the higher baseline R in the D2 strain by itself could possibly account for an increased responsiveness to methacholine. Although the genetic determinants are of great interest for future studies, the focus of the present study is to explore the interactions between genetic influences and differential aging processes in the lung. Since age-dependent changes in R are

dramatic in D2 mice but not in B6 mice (Fig. 2), the results suggest that there is a potent interaction of aging, which plays a substantial role on the genetic regulation of R between the strains. The age-dependent decline in R as a function of PEEP for D2 mice further suggests that a loss of interdependence between the lung parenchyma and the airway tree is one important manifestation of accelerated aging in this strain. This unique aging effect in the lungs of D2 mice is not solely explicated by the greater R observed in this strain at 2 mo of age (Fig. 2C).

In addition to apparent strain and aging effects in the airways, significant strain variation between B6 and D2 mice was evident in the lung parenchyma at 2 mo of age. The strain differences were especially apparent in the P_{EL} (Fig. 1C) and the compliance of the lung at high pressure (Table 1). The reduced P_{EL} in 2-mo-old D2 mice indicated a significantly lower distensibility of the lung parenchyma relative to B6 mice. There was a further reduction in P_{EL} with age in D2 mice, and the strain difference was exaggerated at 20 mo of age. The D2 strain showed a greater age-dependent leftward shift in the deflation curve than the B6 mice (Fig. 1), and there was a further reduction in P_{EL} with age in this strain. Since the age-dependent change in lung volume did not differ between strains, the 60% lower P_{EL} in D2 mice compared with B6 mice at 20 mo represents a volume-independent effect of aging. This strain-specific loss of elasticity with age observed in D2 mice did not occur in B6 mice. As a result, there was also a significant age-dependent increase in FRC in D2 mice. For

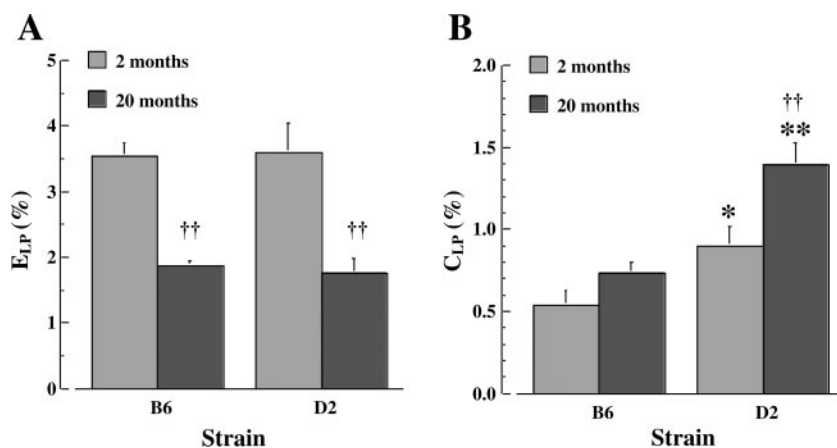


Fig. 4. Elastic fiber density (E_{LP} ; A) and collagen density (C_{LP} ; B) relative to lung parenchyma in B6 and D2 mouse strains. Data are expressed as means \pm SE. * $P < 0.05$, ** $P < 0.01$, D2 vs. B6 at same age; †† $P < 0.01$, 20 mo vs. 2 mo in same strain.

Table 3. Fold changes in gene expression levels related to strain differences in lung extracellular matrix as a function of age

	B6		D2	
	2 mo (n = 3)	20 mo (n = 3)	2 mo (n = 3)	20 mo (n = 3)
<i>Coll1a1</i>	6.4±0.9	1.6±0.1	13.9±2.9*	2.8±0.4§
<i>Col3a1</i>	6.2±1.3	1.8±0.2	20.4±5.2*	2.6±0.3§
<i>Col6a3</i>	4.4±0.6	2.2±0.5	12.9±3.3*	3.0±0.8§
<i>Eln</i>	2.9±0.1	1.4±0.2	8.5±3.4	1.5±0.2‡
<i>Mmp9</i>	2.2±0.6	6.3±1.6	3.3±0.5	21.5±7.6*‡
<i>Mmp12</i>	1.3±0.2	3.0±0.8	3.1±0.7	1.7±0.3
<i>Timp1</i>	1.3±0.1	2.3±0.2‡	2.7±0.1†	1.7±0.4
<i>Timp2</i>	1.4±0.2	1.6±0.3	2.2±0.2	1.6±0.5
<i>Timp3</i>	1.4±0.4	1.6±0.3	2.1±0.4	1.9±0.2
<i>Timp4</i>	1.1±0.1	2.9±0.5§	2.1±0.2	2.8±0.4

All values are expressed as means ± SE. Genes: *Coll1a1*, *Col3a1*, and *Col6a3*, procollagens I, III, and VI; *Eln*, elastin; *Mmp9* and *Mmp12*, matrix metalloproteinases 9 and 12; *Timp1*, *Timp2*, *Timp3*, *Timp4*, tissue inhibitor of matrix metalloproteinase-1, -2, -3, and -4. * $P < 0.05$, and † $P < 0.01$, D2 vs. B6 at same age; ‡ $P < 0.05$, and § $P < 0.01$, 20 mo vs. 2 mo in same strain.

example, the rise in FRC in D2 mice with age is threefold greater than in B6 mice (93% in D2 vs. 30% in B6). Therefore, not only do genetic determinants regulate volume-independent differences between B6 and D2 strains, but also the lung parenchyma of D2 mice is more vulnerable to the effects of accelerated aging compared with B6 mice.

Elastin and collagen are important structural proteins composing the alveolar structure and the lung parenchyma and are most important in determining the mechanical properties of lung (35, 37). Thus it is reasonable to postulate that strain differences in elastin and/or collagen with senescence between B6 and D2 might also contribute to the accelerating emphysematous-like changes in D2 mice. Traditionally, elastic fiber degradation was considered a key factor contributing to loss of elastic recoil in the pathogenesis of aging and emphysema (20, 24, 28). However, the strain variation that we observed in elastic recoil pressure as a function of age (Fig. 1C) was not accompanied by parallel changes in E_{LP} (Fig. 4A). Collectively, these results demonstrated that E_{LP} was not the only factor or even a primary factor in the greater loss in elastic recoil found in the D2 strains. Other studies (3, 14, 21) have shown similar inconsistencies. Taken together, these studies make it clear that the changes in lung mechanics involve a complex interaction between several structural proteins in the extracellular matrix.

Consistent with this conjecture, we found age-dependent lung changes unique to D2 mice, particularly in the loss of lung tissue (T_D) and the increase in collagen content in the lung parenchyma at 20 mo of age. This loss of lung tissue with increased collagen content in parenchyma must have some effect on the aging differences in lung mechanics at 20 mo in D2 compared with B6 mice. Although age-related changes in collagen content of human and animal lungs have been reported (25, 39), the results have varied widely. In human lungs, various environmental factors including pollutant and cigarette smoke exposures may have affected the aging process. Several studies have shown that D2 inbred mice are more susceptible to lung pathophysiological effects following exposure to cigarette smoke (4) and bleomycin (7) than B6 mice. In the

present study, we found that collagen content increased significantly with age between 2 and 20 mo in D2 mice but not in B6 mice (Fig. 4B). Chung and colleagues (7) showed that D2 mice were uniquely susceptible to bleomycin-induced increases in collagen content, leading to prolonged fibrosis compared with B6 mice. These results strongly suggested that genetic determinants lead to greater susceptibility to collagen deposition and persistent fibrosis. The present study suggests that similar changes may occur in D2 mice with senescence.

The disparity between the D2 and B6 strains of mice in senescent-dependent lung changes is likely attributable to a complex interaction between genetic predisposition and ongoing aging processes. To begin to address this, we tested whether there were strain-specific age-dependent differences in ECM-related gene expression levels. We observed age-dependent downregulation in gene expression levels for *Eln*, *Coll1a1*, *Col3a1*, and *Col6a3* genes in both strains, but the extent of downregulation was more dramatic in D2. These findings are consistent with the hypothesis that organ-specific genes modulate the rate of aging, and decreased gene expression levels of structural proteins in the ECM can parallel accelerated aging specific to that organ. That is, the slowing of ECM protein synthesis is one of the most commonly observed biochemical changes during aging (29). From the present study, the results indicate that the lung of D2 mice is more susceptible to accelerated aging than B6 mice. Although we cannot show a causal link, it is clear that this accelerated aging of the lung is correlated with the downregulation of *Eln*, *Coll1a1*, *Col3a1*, and *Col6a3* gene expression levels in D2 mice. One additional factor that can also affect the shape of the P-V curve is surface tension. We did not measure surfactant levels in the strains and are unaware of published data that show changes in surfactant in the aging lung or among different mouse strains. Thus the potential importance of age- and strain-dependent alterations in surfactant remains to be determined. However, to the extent that such changes exist, it is uncertain how this factor might influence the observed age-dependent changes.

In general, protein turnover is hindered by an age-dependent decrease in proteolytic activity (29). For the lung, matrix metalloproteinases (Mmps) are an important family of proteolytic enzymes and can be broadly classified on the basis of substrate specificity (9, 42). The key characteristic of Mmps is their ability to degrade structural proteins of the ECM, and *Mmp9* and *Mmp12* play a significant role in the development of lung destructive diseases, such as emphysema (17, 22). Clinical data have also shown elevated *Mmp9* and *Mmp12* levels in bronchoalveolar lavage fluid as well as in bronchial biopsies of chronic obstructive pulmonary disease patients when compared with controls (8, 15). In the present study, we found that the gene expression levels of *Mmp9* were significantly ($P < 0.05$) increased with age only in 20-mo-old D2 mice and not in B6 mice. That is, the lungs from 20-mo-old D2 mice expressed 6.6 times more *Mmp9* compared with the expression levels in 2-mo-old D2 mice and 3.4 times more than 20-mo-old B6 mice (Table 3). These findings suggest that the proteolytic activity of *Mmp9* may be a significant contributing factor in the accelerated aging of the lung in D2 mice. In contrast, the expression levels of *Timp1* and *Timp4* genes were significantly increased in 20-mo-old B6 mice, suggesting that these may provide important inhibitory effects on the age-dependent degradation of the lung in this strain. The results

also show that the gene expression levels of *Mmp12* were not significantly different with age in either strain, although there was a significant ($P < 0.05$) interaction between age and strain; that is, the gene expression of *Mmp12* was increased with age in B6, whereas it was decreased with age in D2 (Table 3). Our findings are consistent with the hypothesis that an imbalance between *Mmp9* and its tissue inhibitors accelerates lung aging and may induce a greater lung tissue remodeling in D2 compared with B6 mice.

In conclusion, our results suggest that there are strain-specific differences in lung senescence between B6 and D2 mice. These data further suggest that robust genetic determinants regulate the rate of age-dependent changes in the lung, with D2 mice demonstrating accelerated aging compared with B6 mice. The physiological changes in R as a function of lung inflation in the D2 mice are most notable and indicate a dramatic age-dependent change in the interdependence between the lung parenchyma and the airways. The decline in the recoil pressure in D2 mice further suggested that the accelerated aging of the lung in D2 mice involves the loss of parenchymal elasticity. While both strains showed similar declines in elastic fiber content, the D2 strain demonstrated a greater age-dependent increase in collagen content. This parenchymal remodeling is a consequence of a complex interaction between genetic predisposition and aging. Since these changes observed in mice mimic those seen in human subjects, these genetic models may be useful in studying specific genetic processes that are generally applicable to the aging mammalian lung.

GRANTS

This study was supported by National Institute on Aging Grant AG-21057 (C. G. Tankersley) and National Heart, Lung, and Blood Institute Grants HL-010342 (C. G. Tankersley) and HL-081205 (S. Biswal).

REFERENCES

- Allen GB, Suratt BT, Rinaldi L, Petty JM, Bates JH. Choosing the frequency of deep inflation in mice: balancing recruitment against ventilator-induced lung injury. *Am J Physiol Lung Cell Mol Physiol* 291: L710–L717, 2006.
- Arriaga AK, Orozco EH, Aguilar LD, Rook GA, Hernandez Pando R. Immunological and pathological comparative analysis between experimental latent tuberculous infection and progressive pulmonary tuberculosis. *Clin Exp Immunol* 128: 229–237, 2002.
- Bachofen H, Schurch S, Urbinelli M, Weibel ER. Relations among alveolar surface tension, surface area, volume, and recoil pressure. *J Appl Physiol* 62: 1878–1887, 1987.
- Bartalesi B, Cavarra E, Fineschi S, Lucattelli M, Lunghi B, Martorana PA, Lungarella G. Different lung responses to cigarette smoke in two strains of mice sensitive to oxidants. *Eur Respir J* 25: 15–22, 2005.
- Burr ML, Phillips KM, Hurst DN. Lung function in the elderly. *Thorax* 40: 54–59, 1985.
- Chan ED, Welsh CH. Geriatric respiratory medicine. *Chest* 114: 1704–1733, 1998.
- Chung MP, Monick MM, Hamzeh NY, Butler NS, Powers LS, Hunninghake GW. Role of repeated lung injury and genetic background in bleomycin-induced fibrosis. *Am J Respir Cell Mol Biol* 29: 375–380, 2003.
- Churg A, Wright JL. Proteases and emphysema. *Curr Opin Pulm Med* 11: 153–159, 2005.
- Elkington PT, Friedland JS. Matrix metalloproteinases in destructive pulmonary pathology. *Thorax* 61: 259–266, 2006.
- Escolar JD, Tejero C, Escolar MA, Montalvo F, Garisa R. Architecture, elastic fiber, and collagen in the distal air portion of the lung of the 18-month-old rat. *Anat Rec* 248: 63–69, 1997.
- Hantos Z, Collins RA, Turner DJ, Janosi TZ, Sly PD. Tracking of airway and tissue mechanics during TLC maneuvers in mice. *J Appl Physiol* 95: 1695–1705, 2003.
- Hantos Z, Daroczy B, Suki B, Nagy S, Fredberg JJ. Input impedance and peripheral inhomogeneity of dog lungs. *J Appl Physiol* 72: 168–178, 1992.
- Hirai T, Hosokawa M, Kawakami K, Takubo Y, Sakai N, Oku Y, Chin K, Ohi M, Higuchi K, Kuno K. Age-related changes in the static and dynamic mechanical properties of mouse lungs. *Respir Physiol* 102: 195–203, 1995.
- Ito S, Ingenito EP, Brewer KK, Black LD, Parameswaran H, Lutchen KR, Suki B. Mechanics, nonlinearity, and failure strength of lung tissue in a mouse model of emphysema: possible role of collagen remodeling. *J Appl Physiol* 98: 503–511, 2005.
- Joos L, He JQ, Shepherdson MB, Connett JE, Anthonisen Pare PD, Sandford AJ. The role of matrix metalloproteinase polymorphisms in the rate of decline in lung function. *Hum Mol Genet* 11: 569–576, 2002.
- Kida K, Fujino Y, Thurlbeck WM. A comparison of lung structure in male DBA and C57 black mice and their F1 offspring. *Am Rev Respir Dis* 139: 1238–1243, 1989.
- Lanone S, Zheng T, Zhu Z, Liu W, Lee CG, Ma B, Chen Q, Homer RJ, Wang J, Rabach LA, Rabach ME, Shipley JM, Shapiro SD, Senior RM, Elias JA. Overlapping and enzyme-specific contributions of matrix metalloproteinases-9 and -12 in IL-13-induced inflammation and remodeling. *J Clin Invest* 110: 463–474, 2002.
- Levitt RC, Mitzner W. Autosomal recessive inheritance of airway hyperreactivity to 5-hydroxytryptamine. *J Appl Physiol* 67: 1125–1132, 1989.
- Martin CJ, Chihara S, Chang DB. A comparative study of the mechanical properties of aging alveolar wall. *Am Rev Respir Dis* 115: 981–988, 1977.
- McCusker K. Mechanisms of respiratory tissue injury from cigarette smoking. *Am J Med* 93: 18S–21S, 1992.
- Mercer RR, Russell ML, Crapo JD. Alveolar septal structure in different species. *J Appl Physiol* 77: 1060–1066, 1994.
- Morris DG, Huang X, Kaminski N, Wang Y, Shapiro SD, Dolganov G, Glick A, Sheppard D. Loss of integrin alpha(v)beta6-mediated TGF-beta activation causes Mmp12-dependent emphysema. *Nature* 422: 169–173, 2003.
- Nagase T, Fukuchi Y, Teramoto S, Matsuse T, Orimo H. Mechanical interdependence in relation to age: effects of lung volume on airway resistance in rats. *J Appl Physiol* 77: 1172–1177, 1994.
- Niewoehner DE. Cigarette smoking, lung inflammation, and the development of emphysema. *J Lab Clin Med* 111: 15–27, 1988.
- Pierce JA, Hocott JB. Studies on the collagen and elastin content of the human lung. *J Clin Invest* 39: 8–14, 1960.
- Pierce RA, Albertine KH, Starcher BC, Bohnsack JF, Carlton DP, Bland RD. Chronic lung injury in preterm lambs: disordered pulmonary elastin deposition. *Am J Physiol Lung Cell Mol Physiol* 272: L452–L460, 1997.
- Pride NB. Aging and changes in lung mechanics. *Eur Respir J* 26: 563–565, 2005.
- Ranga V, Kleinerman J, Ip MP, Sorensen J. Age-related changes in elastic fibers and elastin of lung. *Am Rev Respir Dis* 119: 369–376, 1979.
- Rattan SI. Synthesis, modifications, and turnover of proteins during aging. *Exp Gerontol* 31: 33–47, 1996.
- Reinhard C, Eder G, Fuchs H, Ziesenis A, Heyder J, Schulz H. Inbred strain variation in lung function. *Mamm Genome* 13: 429–437, 2002.
- Reinhardt AK, Bottoms SE, Laurent GJ, McNulty RJ. Quantification of collagen and proteoglycan deposition in a murine model of airway remodeling. *Respir Res* 6: 1–13, 2005.
- Savov JD, Whitehead GS, Wang J, Liao G, Usuka J, Peltz G, Foster WM, Schwartz DA. Ozone-induced acute pulmonary injury in inbred mouse strains. *Am J Respir Cell Mol Biol* 31: 69–77, 2004.
- Schmittgen TD, Zakrajsek BA, Mills AG, Gorn V, Singer MJ, Reed MW. Quantitative reverse transcription-polymerase chain reaction to study mRNA decay: comparison of endpoint and real-time methods. *Anal Biochem* 285: 194–204, 2000.
- Sherrill DL, Lebowitz MD, Knudson RJ, Burrows B. Longitudinal methods for describing the relationship between pulmonary function, respiratory symptoms and smoking in elderly subjects: the Tucson Study. *Eur Respir J* 6: 342–348, 1993.
- Sly PD, Collins RA, Thammrin C, Turner DJ, Hantos Z. Volume dependence of airway and tissue impedances in mice. *J Appl Physiol* 94: 1460–1466, 2003.
- Soutiere SE, Tankersley CG, Mitzner W. Differences in alveolar size in inbred mouse strains. *Respir Physiol Neurobiol* 140: 283–291, 2004.

37. **Suki B, Ito S, Stamenovic D, Lutchen KR, Ingenito EP.** Biomechanics of the lung parenchyma: critical roles of collagen and mechanical forces. *J Appl Physiol* 98: 1892–1899, 2005.
38. **Tankersley CG, Rabold R, Mitzner W.** Differential lung mechanics are genetically determined in inbred murine strains. *J Appl Physiol* 86: 1764–1769, 1999.
39. **Takubo Y, Hirai T, Muro S, Kogishi K, Hosokawa M, Mishima M.** Age-associated changes in elastin and collagen content and the proportion of types I and III collagen in the lungs of mice. *Exp Gerontol* 34: 353–364, 1999.
40. **Turner JM, Mead J, Wohl ME.** Elasticity of human lungs in relation to age. *J Appl Physiol* 25: 664–671, 1968.
41. **Verbeke EK, Cauberghs M, Mertens Clement J I, Lauweryns JM, Van de Woestijne KP.** The senile lung. Comparison with normal and emphysematous lungs. I. Structural aspects. *Chest* 101: 793–799, 1992.
42. **Visse R, Nagase H.** Matrix metalloproteinases and tissue inhibitors of metalloproteinases: structure, function, and biochemistry. *Circ Res* 92: 827–839, 2003.
43. **Whitehead GS, Walker JK, Berman KG, Foster WM, Schwartz DA.** Allergen-induced airway disease is mouse strain dependent. *Am J Physiol Lung Cell Mol Physiol* 285: L32–L42, 2003.

